Image potential states and electronic structure of Na/Cu(111)

G. Butti,[1,2,*] S. Caravati,[1,2] G. P. Brivio,[1,2] M. I. Trioni,[2] and H. Ishida[3]
[1]*Dipartimento di Scienza dei Materiali, Università di Milano-Bicocca, Via Cozzi 53, 20125 Milano, Italy*
[2]*Istituto Nazionale per la Fisica della Materia, Università di Milano-Bicocca, Via Cozzi 53, 20125 Milano, Italy*
[3]*College of Humanities and Sciences, Nihon University, Sakura-josui, Tokyo 156-8550, Japan*
(Received 22 April 2005; revised manuscript received 1 July 2005; published 1 September 2005)

We report a density functional theory investigation of the electronic structure of a monolayer of Na adsorbed on a Cu(111) substrate. We approach this problem by taking into account a truly semi-infinite substrate within the embedding Green function method, which allows one to clearly distinguish surface states from bulk projected ones and to describe them with high accuracy. The quantum-well state induced by Na adsorption is discussed and compared with the surface state of the clean Cu(111) surface. By suitably modifying the method, we are able to study image potential induced states which are normally not available in standard density functional theory calculations. In our approach these states are fully accounted for by introducing the image tail in the effective potential. The theoretical results are compared with experiments when available, for both the clean metal surface and the adsorbate system.

DOI: 10.1103/PhysRevB.72.125402 PACS number(s): 73.20.At, 73.21.Fg, 73.61.At

I. INTRODUCTION

Investigations of alkali adatoms on metal surfaces have been performed for quite a long time.[1,2] Photoemission experiments of alkali overlayers on metal surfaces, and in particular single-photon photoemission (1PPE),[3] inverse photoemission (IPE),[4] and two-photon photoemission (2PPE) (Refs. 3, 5, and 6) studies of alkali adatoms, have been carried out recently, together with several theoretical calculations.[7–14] In fact, those systems are benchmark ones for the study of the basic features of chemisorption processes, such as the charge redistribution and the electronic structure modifications occurring upon adsorption. In this respect the interplay among the projected bulk band structure, the clean surface-specific features, and the alkali atom states plays a crucial role in the atom-surface and adatom-adatom lateral interactions.[15] Na/Cu(111) is a system of particular interest, since the projected band structure of the Cu(111) face displays a wide energy gap at the $\bar{\Gamma}$ point in the surface Brillouin zone (SBZ), where no bulk states are allowed. This condition is equivalent to the presence of a potential barrier toward the substrate preventing surface electronic states from propagating in the bulk region and allowing for the study of the properties of a nearly two-dimensional (2D) electron gas. As shown by experimental investigations, this particular condition generates *quantum-well states*[16] (QWS) within the Na adlayer. An appealing feature of these states is the energy position tunability in the spectrum found by varying the amount of adsorbed sodium.[6,12]

The first density functional theory (DFT) investigations of such adsorbates were carried out on simple metal substrates. They were modeled as jellium in the works by Salmi[7] and Ishida.[8,9] Such calculations led to great progress in the understanding of the alkali-metal adsorption mechanism beyond the Gurney paradigm.[17] At the same time Na/Al(111) was investigated, taking into account also the substrate atomistic structure. This was done both within a pseudopotential approach by Chulkov and Silkin,[10] and a full-potential framework by Benesh and Hester,[11] which focused on the lateral interactions between Na adatoms. Later on, the theoretical analysis was refined by works of Scheffler's group characterizing the surface morphology of the system[18] and its electronic structure.[13] DFT calculations of Na on a periodic Cu(111) surface were recently performed by Carlsson and Hellsing[14] within a plane-wave pseudopotential supercell approach. These authors studied structural properties, such as site preference and bond geometry of the Na adatom, and described the electronic properties of the system. They concentrated on the QWS existing just below the Fermi level and characterized it by comparing the band structure of the Na/Cu system with that of the clean Cu surface and of a freestanding Na monolayer.

The aim of our work is to provide an improved theoretical description, based on first-principles (DFT) calculations within the Green function embedding technique,[19,20] of the electronic properties of Na/Cu(111). We expect to improve on previous results, describing surface-specific features with the greater accuracy provided by the treatment of a semi-infinite substrate allowed by the embedding approach. In addition, we determine image potential induced states, which have been extensively investigated experimentally[3,5,6] and have been recently addressed also from the theoretical point of view.[21]

This paper is organized as follows: In Sec. II we present a brief overview of the method, especially regarding the treatment of image potential induced states within DFT. Section III is divided into an introductory part, and two subsections which deal with the QWS and with image states, respectively. Finally, the last section is devoted to conclusions.

II. THEORETICAL FRAMEWORK

The present calculation is based on the embedding method introduced by Inglesfield[19] to study localized perturbations in infinite systems. In particular, we adopt the implementation by Ishida[20,22] for the treatment of realistic solid

surfaces. Within this framework we consider a system which is infinite, periodic in the xy surface plane but nonperiodic along the surface normal direction z. We define a finite region along z, the so-called embedded region, determined by the volume in which the perturbation due to the surface is well screened. The problem is then solved in such a region only. For a metallic Cu substrate, this implies considering the two topmost Cu layers on the bulk side. Since adsorption of alkali metal atoms on transition metals causes a considerable reduction of the work function, we expect a slow decay of the surface charge density toward vacuum. So, we embed a vacuum region extending for 12 a.u. The calculation is carried out solving a Kohn-Sham (KS)-type equation in the DFT framework, using a Green function description and a full-potential linearized augmented plane-wave (FLAPW) method. Additional terms, called "embedding potentials" and acting as a sort of generalized boundary conditions, appear in the KS Hamiltonian accounting for the presence of the semi-infinite substrate. These potentials are nonlocal and energy dependent, but only their values at the embedding surfaces enter the Hamiltonian. We recall that the embedding potential is defined as the surface inverse of the Green function of the unperturbed substrate over the embedding surface, which is equivalent to the logarithmic derivative of the solutions of the Schrödinger equation at a given energy.[19] The embedding potential at the vacuum region is usually determined analytically from the Green function calculated for a constant potential.[23] Details regarding this method are reported in Refs. 20 and 22.

The implementation presented in this paper has the additional capability of treating image potential induced states. Indeed standard DFT is known not to be able to reproduce the correct asymptotic behavior of the effective potential, V_{eff}, toward vacuum. This is a consequence of the local or semilocal approximations commonly used for the evaluation of the exchange and correlation functional, which determine an exponential asymptotic decay of the potential outside a surface, instead of the correct imagelike behavior $V(z) \sim -1/4z$. In order to restore this property, one possibility is going beyond DFT, as shown by the pioneering work of Eguiluz *et al.*,[24] recently applied to semi-infinite jellium, within the framework of the embedding method, by Fratesi *et al.*[25] Following such a strategy, however, implies a dramatic increase in the computational effort, making the treatment of realistic metal surfaces still a very demanding task. An alternative approach to the study of image potential induced states is the one developed by Nekovee and Inglesfield,[26,27] which exploits the nonperiodicity of the embedding method in the z direction. Indeed, the embedding potential replacing the semi-infinite vacuum can be calculated taking into account the correct form of the asymptotic potential decay. This task requires computation of the logarithmic derivative of outgoing solutions of the Schrödinger equation in the presence of a decaying potential. This quantity is easily calculated by performing a numerical integration of the Schrödinger equation itself. Such an embedding potential replaces the usual one, calculated analytically as discussed above. In order to avoid any discontinuity at the vacuum embedding surface, the effective potential V_{eff} inside the outermost part of the embedded region[28] is obtained by gradually mixing the effective potential of the KS equation with the model potential of the form $-1/4|z-z_{im}|$ (z_{im} being the image plane position). In particular, V_{eff} is defined as

$$V_{eff}(z) = [1 - I_z(a,b)]V_{eff}^{\mathrm{KS}}(z) + I_z(a,b)\frac{-1}{4|z-z_{im}|}, \qquad (1)$$

where $I_z(a,b)$ is an incomplete beta function, but in principle it could be replaced by any monotonic, smoothly varying function in the $[0,1]$ range. The shape of the incomplete beta function is finely tuned by suitably setting the a,b parameters; their value is expected to affect the shape of V_{eff} and therefore slightly modify the results of the calculation. However, we verified that for a range of values of a,b the description of image states and of the electronic properties is unaffected. Let us remark that in this approach we do not evaluate the image potential itself, but simply account for the effect of its presence; hence, the position of the image plane is part of the input data for our calculation. In order to obtain it, we identified two possible strategies. The first one takes advantage of the lack of periodicity of the system in the direction normal to the surface, so that it is easy to apply an external electric field normal to the surface plane.[29,30] Consequently, it is possible to calculate the centroid of the field-induced charge distribution which corresponds to the position of the static image plane, z_{im}, as originally stated by Lang and Kohn.[31] An alternative way of determining z_{im} consists of defining a surface model potential barrier, which is expressed as a function of several parameters, one of which is z_{im} itself. The shape of such a model potential is then fitted to a set of some physical observables, such as the position of the first image state in the Rydberg series or the exact energy gap. In this work we have adopted the model potential proposed in Ref. 21 to determine the z_{im} value. These two methods produce slightly different results, but we observe that those obtained with the second one are closely related to the experimental results. In particular, this method allows one to well describe the first state in the Rydberg series, which is located in a spatial region where the surface potential has not yet reached its asymptotic behavior. Since comparison with experiments is a primary objective of this work, all the reported results for the image plane coordinate are worked out in this way. In particular, we used $z_{im}=2.30$ a.u. for the clean Cu(111) surface and $z_{im}=3.67$ a.u. for the Na-covered one; these coordinates are referred to the position of the topmost layer in both systems.

Regarding the main parameters of the calculation, the Green function was expanded using 10.24 Ry as a cutoff for the plane wave in the interstitial part. We set $l_{max}=9$ for the spherical expansion inside the muffin tins (MT), whose radii were chosen to be the same, namely $r_{\mathrm{MT}}^{\mathrm{Na}}=r_{\mathrm{MT}}^{\mathrm{Cu}}=2.4$ a.u. The surface Brillouin zone (SBZ) for the clean Cu(111) surface, was sampled by a 16×16 regular mesh which was reduced to a set of 51 independent $\mathbf{k}_{\parallel}$ points; for adsorbed Na the SBZ becomes nine times smaller (see Sec. III) and was sampled with a 6×6 mesh consisting of ten independent $\mathbf{k}_{\parallel}$ points. All the results presented in this work are obtained within a generalized gradient approximation for the exchange and

TABLE I. Comparison between the calculated and the experimental work functions.

System	Calculated (eV)	Experimental (eV)
Clean Cu(111)	4.89	4.93 (Ref. 36)
(2×2) Na/Cu	1.92	2.1 (Ref. 37)
$(3/2\times3/2)$ Na/Cu	2.96	2.77 ± 0.03 (Ref. 6)

correlation functional as proposed by Perdew, Burke, and Erznerhof (GGA-PBE).[32]

III. RESULTS

A. General features

The experimental investigations on the Na/Cu(111) system via low-energy electron diffraction (LEED) (Refs. 4 and 33) and low-temperature scanning tunneling microscopy (STM) (Ref. 34) report the existence of a $p(3\times3)$ reconstruction with four Na atoms per unit cell at monolayer (ML) coverage (0.44 ML nominal coverage). In the rest of this paper, we will refer to such a structure as the $(3/2\times3/2)$. In the submonolayer regime the existence of an ordered phase is somewhat still debated: ring structures appear in the LEED experiment by Tang *et al.*,[33] indicating the absence of long-range order in the Na film. On the contrary in the experiment by Dudde *et al.*[4] a clear 2×2 pattern is reported, which should indicate the existence of a phase corresponding to a coverage of 0.56 ML (0.25 ML nominal). In their recent work, Kliewer and Berndt[34] try to reconcile these two observations, proposing the coexistence of both these phases in different fractions of the sample for coverages below 1 ML.

In this work we analyze the differences between the clean Cu(111) surface and the 1 ML Na-covered one. We also performed calculations for the 0.56 ML case. The structural properties of all these phases were determined by Carlsson and Hellsing in Ref. 14. In their work they optimized the geometry of the system, determining the bulk equilibrium lattice constant and performing subsequent surface optimizations (Cu surface relaxation and position of adsorbed sodium) on the basis of that parameter. We approached this problem in a different way. We observe that the structural properties determined by DFT are often under- or overestimated by a small amount (around 2% in most cases), depending on the exchange-correlation functional and that in some cases the electronic properties are very sensitive to the chosen configuration. In particular, the Na adsorption coordinate, together with the adatom effective charge, defines the induced dipole moment, which determines the amount of the work function decrease.[35] Therefore, in order to produce the best input configuration for our computation of the electronic properties, we decided to take the experimentally determined structural data whenever available, and, only when they are not, to calculate the system coordinates. The comparison between the calculated and the experimental work functions in Table I shows an excellent agreement for the clean Cu(111) surface. On the other hand, the Na-adsorbed systems present a small discrepancy.

Let us now focus on the electronic structure of the system. In Fig. 1 we report both the density of states (DOS), integrated in the whole SBZ, for the clean Cu(111) surface (right panels) and for the Na-covered system (left panels). In this plot we distinguish between the contributions from the MT (represented by the thicker lines) and from the interstitial or the vacuum region (thinner lines). The reference energy is the Fermi level of the Cu substrate. In the Na/Cu(111) system, for each atomic species there are atoms which are inequivalent by symmetry; however, the differences for the atoms in the same layer are so negligible that we decided to report only the DOS in a single MT per layer. In panel (a) we show the DOS in the inner Cu layer, while (b) shows that of the topmost one. The MT contribution is clearly the dominant one because of the close-packed structure of Cu. We note that the line shape of the DOS around a Cu atom is very

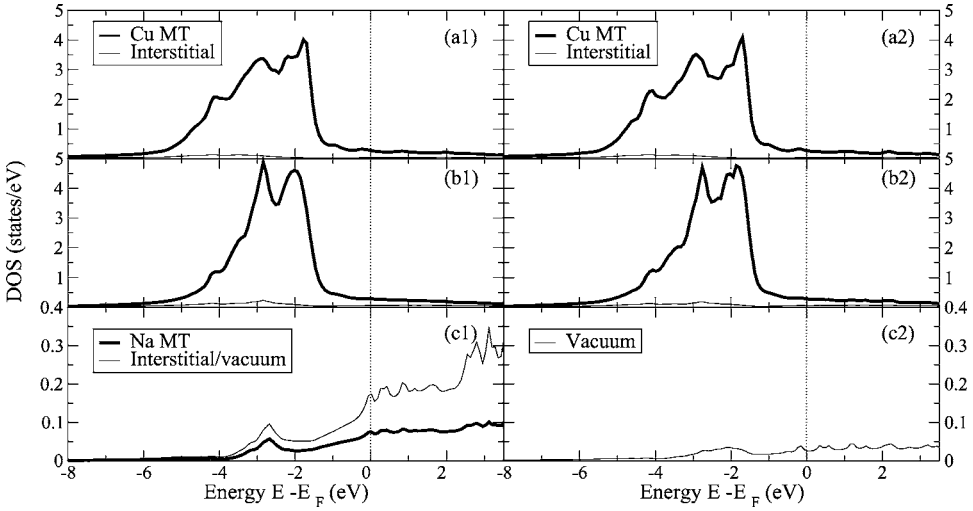

FIG. 1. Calculated DOS in different volumes. The left plots display the $(3/2\times3/2)$ Na/Cu(111); the right ones show the clean Cu(111) surface; (a1,a2) second Cu layer; (b1,b2) top Cu layer; (c1) Na layer; (c2) vacuum contribution. Thick lines refer to the DOS evaluated in the MT volume, thinner ones for the interstitial or vacuum regions.

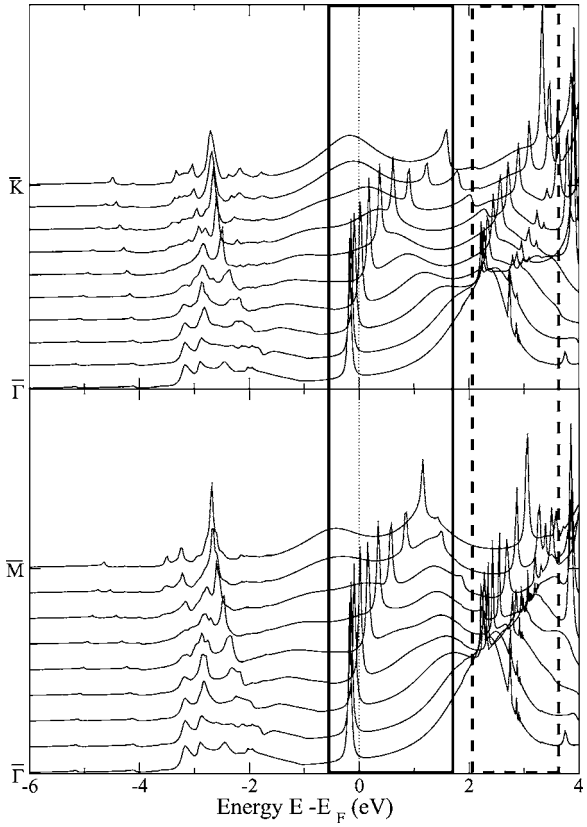

FIG. 2. Dispersion of the DOS for the Na/Cu(111) system, evaluated inside one of the two inequivalent Na MTs along two different high-symmetry paths: $\overline{\Gamma K}$ (above) and $\overline{\Gamma M}$ (below). The thick solid and the dashed lines enclose the dispersion of the QWS and of the image states, respectively.

similar in both systems. Hence, we can infer that the presence of Na does not cause significant modification in the electronic structure of the substrate. In panel (c) we compare the DOS in the Na MT and the vacuum region (on the left) to the one evaluated in the same volume on the clean Cu surface. In this case the contribution from the vacuum and interstitial volumes dominates over the MT one, suggesting that the Na valence electron is much delocalized at the Na-Cu interface.

B. Quantum-well state

The analysis of the DOS in the whole SBZ cannot, in general, account for any intrinsic surface features. These may either be sharp (discrete) ones as a function of energy or display a finite width (resonances), and they usually follow a dispersion law as a function of $\mathbf{k}_{\parallel}$. We thus proceed by calculating the DOS at a given $\mathbf{k}_{\parallel}$, along two high-symmetry paths, $\overline{\Gamma K}$ and $\overline{\Gamma M}$, in the SBZ corresponding to the $p(3\times3)$ structure. In Fig. 2 we display the DOS integrated in one of the two inequivalent Na MTs present in the $3/2\times3/2$ reconstruction of Na/Cu(111). It is to be noted that the energy band gap of the clean Cu(111) at $\bar{\Gamma}$ is not seen in this figure due to the SBZ folding. In the valence range the number of states is however very small, due to the charge redistribution process occurring upon adsorption.

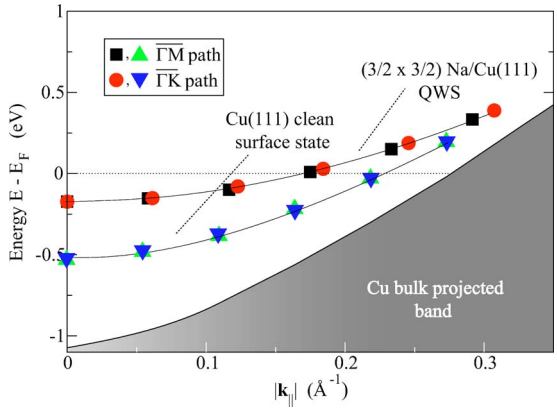

FIG. 3. (Color online) Comparison of the dispersion of the QWS with the clean Cu(111) surface SS along both paths. Squares and upward triangles refer to $\overline{\Gamma M}$, circles and downward triangles to $\overline{\Gamma K}$. The continuous lines are guides for the eye only and do not represent fitting procedure results.

As already shown by Carlsson and Hellsing,[14] and confirmed by our calculation, there is a substantial charge depletion around the Na atom while charge piles up at the interface with the Cu substrate. This polarization creates a dipole moment whose main effect is the work function reduction. Because of this charge transfer, the Na $3s$ resonance is shifted above the Fermi level. In the $\mathbf{k}_{\parallel}$-resolved DOS in Fig. 2 this resonance is nearly degenerate in energy with the $3p$ one, forming the broad structure between 1 and 3 eV at the $\bar{\Gamma}$ point. In Fig. 2 the dispersion of the discrete surface states (the QWS and the image ones) is presented in the region enclosed by the thick lines (solid and dashed, respectively). We remark that the QWS, at this Na coverage, is occupied at the $\bar{\Gamma}$ point, in agreement with previous results.[14,38] This state is clearly identified in the DOS as a sharp peak emerging from the Na valence band. Note that we have introduced a small, yet finite, imaginary part of the energy (27 meV) in order to detect a delta-function-like QWS with a finite sampling of the energy axis. Consequently, this QWS displays a linewidth which has been artificially broadened in order to detect it with a finite sampling of the energy axis. In addition, we point out that, differently from a supercell calculation,[14] the use of a semi-infinite substrate allows for a more accurate description of surface states. Indeed, owing to the presence of only one surface, we do not observe any splitting of the overlayer states due to the spurious interactions across the Cu slabs. This splitting, whose extent is $\mathbf{k}_{\parallel}$ dependent, is usually treated by an averaging procedure which may affect the overall accuracy of the result. From the results of Fig. 2 we can extract the dispersion of the QWS, obtain its binding energy at $\bar{\Gamma}$, and calculate via a simple fit its effective mass along both paths. Those quantities are available by examining Fig. 3 in which we also show the dispersion of the Shockley state (SS) of the clean Cu(111) surface, for comparison. The physics underlying the just-mentioned Shockley state and the QWS of Na/Cu(111) is essentially the same;[16] both are originated by confinement between the potential barrier on the vacuum side and an en-

TABLE II. Key features of the bound discrete states: The SS of clean Cu(111) and the QWS of the $(3/2\times3/2)$ Na/Cu(111) system. The reference energy is the Fermi level.

	Calculated	Experimental
Clean Cu(111)-SS		Ref. 41
Energy (eV)	−0.526	−0.434±0.002
		−0.445[a]
k_F (Å^{-1})	0.228	0.222±0.001
Effective mass (m_e)	0.394[b]	0.43±0.01
$(3/2\times3/2)$ Na/Cu(111)-QWS		Ref. 38
Energy (eV)	−0.173	−0.127
k_F (Å^{-1})	0.170	~0.15
Effective mass (m_e)	0.638	0.70±0.04

[a]Reference 42.
[b]Evaluated for $k_\parallel \leqslant k_F$.

ergy gap of forbidden bulk states on the substrate one. Obviously, when adsorbed Na is present, the boundary condition (i.e., the shape of the potential) at vacuum is modified together with the extension of the well in the z direction. For this reason these two states display different features. Since they are due to a *quasi*–2D distribution of charge confined in a region where the planar corrugation of the potential is low, they are often assumed to have nearly free electron character in the surface plane. Consequently, one could determine their effective mass from a free-particle dispersion in $|\mathbf{k}_\parallel|$. However, this is only an approximation which may hold only for small values of $|\mathbf{k}_\parallel|$, or even fail as for surface states with energy close to the band edge. In this case the state decays slowly into the substrate.[39] Hence, a considerable portion of the charge distribution of such a state is located in the subsurface layers where the corrugation of the potential is larger. The fit of the QWS dispersion with the free-particle law in the $|\mathbf{k}_\parallel|$ range reported in Fig. 3 is excellent ($\chi^2 \approx 10^{-8}$), corresponding to an effective mass $m^*_{QWS}=0.638\ m_e$. In addition, this value does not change by varying the $|\mathbf{k}_\parallel|$ range over which the fitting is performed. On the other hand, the quality of the fit of the effective mass of the Cu(111) SS is worsened significantly without a linear term ($\chi^2 \approx 10^{-6}$), and one obtains different effective masses by varying the $|\mathbf{k}_\parallel|$ range. Their values go from $m^*_{SS}=0.445\ m_e$ at full range to $m^*_{SS}=0.303\ m_e$ considering only a minimal set of $\mathbf{k}_\parallel$ points around $\bar{\Gamma}$. In comparing with experiments, it is therefore important to consider the wave-vector range of the fit. Results of such a comparison, together with a summary of the features of these states, are reported in Table II. We note that in our calculation both the QWS and, to a larger extent the SS, are overbound. Recall that the decay of such states (in particular of the SS) into bulk is considerably slow; this causes the presence of a charge tail outside the embedded region which could modify the effective potential with respect to the unperturbed bulk substrate.[40] In order to further characterize these surface states, we calculated the distribution of the charge density at a given $\mathbf{k}_\parallel$, in particular at the $\bar{\Gamma}$ point. The result is reported in Fig. 4; the plane of the plot is normal to the surface and contains both the Cu and the Na atoms. In this plot we retrieve most of the features that have already been described: for example, we note the low corrugation in the in-plane direction and the localization of the SS and QWS on the surface layers. For the clean Cu(111) surface, it is well known that the SS has a p_z orbital character. In fact, by comparing the charge oscillations with the atomic positions in Fig. 4 (represented by the spheres in the plot), we observe that the charge has minima at the atomic coordinates. The charge density at the $\bar{\Gamma}$ point of the QWS of Na/Cu(111) also shows this behavior. An excellent agreement with the results by Chulkov *et al.*[21] is found for the clean Cu(111) SS. For the Na/Cu QWS our calculation shows that the position of the outermost charge density maximum is outside the sodium layer, in agreement with results by Carlsson and Hellsing[14] but in contrast with what is reported in Ref. 21, where such a position coincides with the Na adatom coordinate.

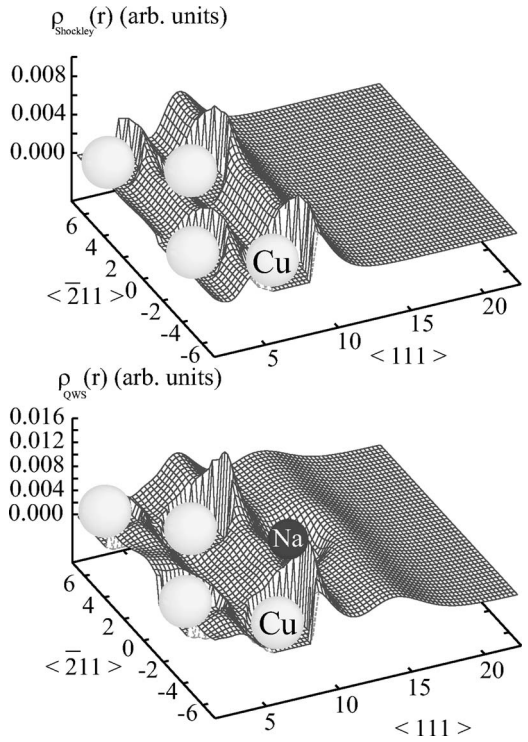

FIG. 4. Charge density plot at $\bar{\Gamma}$ point of the discrete bound states. The upper panel shows that of the SS of the clean Cu(111) surface, while the lower panel shows that of the QWS in the Na-covered surface.

C. Image states

We will now focus on the unoccupied part of the spectrum; in particular, we will concentrate on the image potential induced states which have already been the subject of investigations, mainly from the experimental point of view.[5,6] Following the procedure outlined in Sec. II, the Rydberg series of image states clearly appears in our DOS. In principle, we can obtain the full series by judiciously choosing a suitable imaginary part of the energy in order to

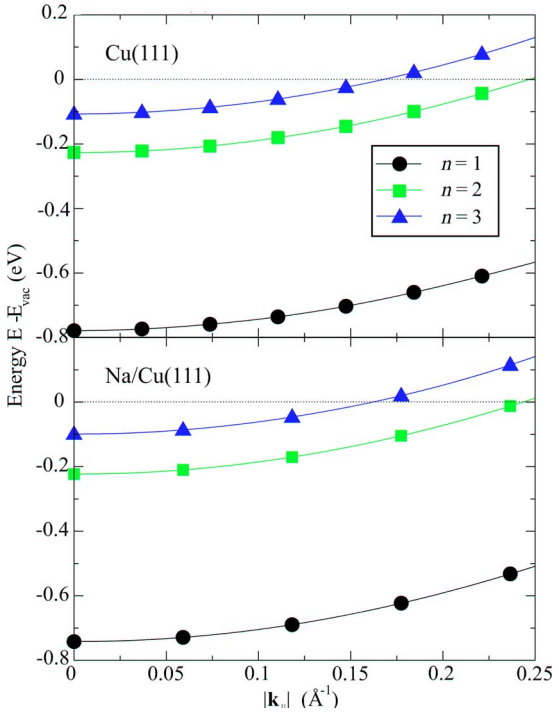

FIG. 5. (Color online) Dispersion of the first three image states of the clean Cu(111) surface (top panel) and of the $(3/2\times3/2)$ Na/Cu(111) system (bottom panel). $\mathbf{k}_{\parallel}$ is sampled along the $\bar{\Gamma}\bar{M}$ path.

resolve the states accumulating at the vacuum level. However, in the following we will concentrate only on the first three states ($n=1,2,3$), which are the ones that have been described experimentally. From the results of Fig. 2, we extract the position of the peaks of Na/Cu(111) and report them in Fig. 5, where we also display those for the clean Cu(111) for comparison. The key features characterizing these states are summarized in Table III. We note that the only image state somewhat affected by the substrate is the lowest one of the Rydberg series, $n=1$. Indeed, the maximum of the probability density of the higher states is located at a distance from the solid which grows quadratically as a function of n. Therefore, the larger part of the wave functions of these states lies in a region far away from the surface plane, where the shape of the effective potential is almost independent of the substrate. We obtain an excellent agreement between the experimental binding energies and those of our calculation: differences are of the order of a few hundredths of an electron volt, comparable to the uncertainty of the measurements. We also determined the effective mass of these states, which is very close to unity in all cases, the effective potential being almost flat in the region outside the surface where they are mostly located. Unfortunately, we could not report a comparison of the effective mass of these states with experiments: to our knowledge, the only study on such a topic for Na/Cu was reported by Fischer *et al.*,[3] stating that it is possible to fit both the QWS and the first image state with the same effective mass ($m^*=1.3\ m_e$). This claim is in disagreement with subsequent works[37,38] and therefore can-

TABLE III. Key features of the first three image states for the clean Cu(111) surface and the $(3/2\times3/2)$ Na/Cu(111) one.

		Calculated		Experimental
System	State	Energy (eV)	Effective mass (m_e)	Energy (eV)
Cu(111)	$n=1$	−0.779	1.10	−0.82±0.05[a]
Clean surface	$n=2$	−0.226	1.02	−0.27±0.07[a]
	$n=3$	−0.107	1.00	
$(3/2\times3/2)$	$n=1$	−0.742	1.02	−0.72±0.03[b]
Na/Cu(111)	$n=2$	−0.223	1.01	−0.27±0.03[b]
	$n=3$	−0.099	1.00	−0.13±0.04[b]

[a]Reference 43.
[b]Reference 5.

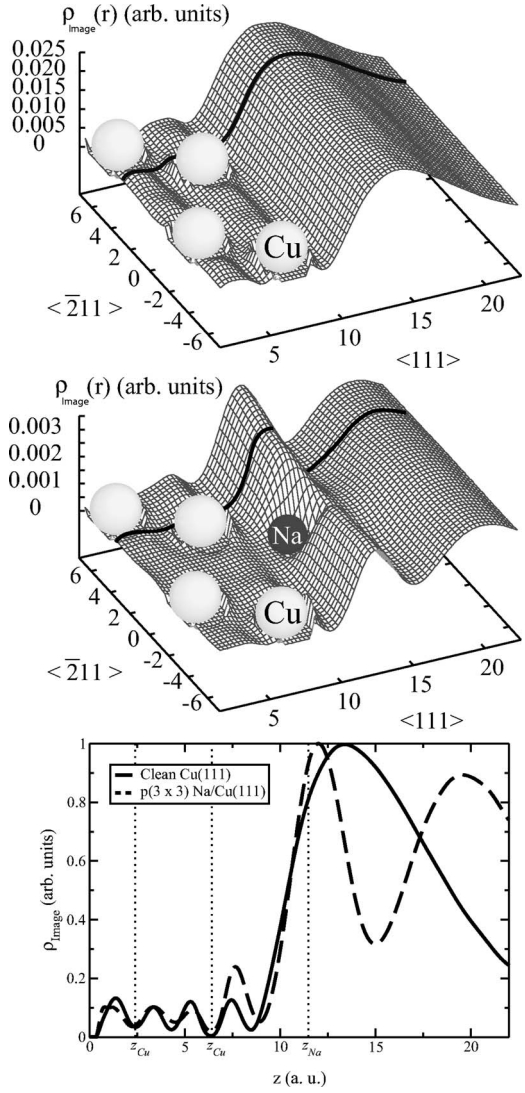

FIG. 6. Charge density plots at $\bar{\Gamma}$ of the first image state of the clean Cu(111) surface (top panel) and of the $3/2\times3/2$ Na/Cu(111) system (middle panel). In the bottom panel we compare two sections of these plots taken along a plane which cuts the charge density along the thick solid lines.

not be considered for comparison. A comparison could be done instead with the previous theoretical investigation by Carlsson and Hellsing,[14] where they discuss a "second Na induced band" which should be confronted with our first image state. Although this state is slightly modified by Na adsorption, it is however a common feature of metal surfaces and cannot be ascribed to the Na adlayer. The existing measurements of the effective mass of the image states of the clean Cu(111) surface are rather old and are given with an error bar of the order of one tenth of m_e, making comparison rather meaningless. We also calculated the charge density distribution at $\bar{\Gamma}$ of the first state in the Rydberg series, as plotted in Fig. 6. In the top and in the middle panels we plot the charge density of the first image state of the clean Cu(111) surface and of the $(3/2\times3/2)$ Na/Cu(111) system, respectively. In the bottom panel we compare these two results, with their maxima normalized to unity, by plotting them along a section plane which cuts the plots along the thick solid lines. For the clean Cu(111) surface, such charge density shows a wide maximum located far outside the surface plane at a distance of about 7 a.u. from the topmost copper layer, in agreement with results from model potential calculations.[44] On Na adsorption it displays a more complex structure with two relative maxima. The shape of the outer one very much resembles that of the image state of the clean Cu(111) surface. Such a charge density is located further outside the topmost (Na) layer at a distance of about 8 a.u. The second structure, closer to the Na adlayer, is more peaked and its center of gravity shifted by about 0.5 a.u. toward the vacuum with respect to the adlayer coordinate. In order to analyze why these two states present different features, we must take into account that the first image state appears as a sharp structure superimposed to the broad one representing the 3*s* and 3*p* Na resonant states (see Fig. 2). Consequently, the two structures of the charge distribution in Fig. 6 should be interpreted differently: the outer one represents the image state, while that near the Na layer is mainly due to the overlayer states. However, a clear distinction is difficult to make, though we can state that a weak interaction between them causes some hybridization which partially contributes to the inner structure between the two relative minima. We conclude that in the two systems the charge density of the first image state is essentially located at a constant distance from the last atomic layer (the small shift of 1 a.u. is related to the difference in the image plane position). We also point out that in our approach we are able to account for a possible interaction between the image and substrate states. Although this coupling is always very weak because of the small overlap between wave functions, it is however an important issue which explains the small differences displayed by these states for different substrates.

IV. CONCLUSIONS

In this work we present the results of calculations of the electronic states spatially confined at the clean Cu(111) surface, focusing on the modifications induced by adsorption of 1 ML of Na. In this case we studied the features of the QWS, below the Fermi level at the $\bar{\Gamma}$ point, and we compared it with the SS of the Cu(111) clean surface. We also analyzed the features of the first three image states in both systems. For each of them we determined the binding energy, the effective mass, and the spatial localization. In all cases, we report a very good agreement with the highly resolved experimental data obtained from previous studies. With respect to the previous theoretical investigation by Carlsson and Hellsing,[14] we point out that we only found one Na-induced state, the QWS, while the second band in their work should be attributed to an image state, which cannot be computed in their approach. In this respect, our results show that the embedding method is particularly suitable to achieve a detailed description of image potential induced states. Our phenomenological implementation within the embedding framework allows one to obtain them considering a realistic substrate (with a nontrivial $\mathbf{k}_\parallel$ dependence) at a computational cost which is far lower than that of a GW calculation.

ACKNOWLEDGMENTS

This work was funded in part by the EU's 6th Framework Program through the NANOQUANTA Network of Excellence (NMP4-CT-2004-500198).

*Electronic address: gabriele.butti@unimib.it

[1] R. D. Diehl and R. McGrath, Surf. Sci. Rep. **23**, 49 (1996).
[2] R. D. Diehl and R. McGrath, J. Phys.: Condens. Matter **9**, 951 (1997).
[3] N. Fischer, S. Schuppler, R. Fischer, Th. Fauster, and W. Steinmann, Phys. Rev. B **43**, R14722 (1991).
[4] R. Dudde, L. S. O. Johansson, and B. Reihl, Phys. Rev. B **44**, 1198 (1991).
[5] N. Fischer, S. Schuppler, R. Fischer, Th. Fauster, and W. Steinmann, Phys. Rev. B **47**, 4705 (1993).
[6] N. Fischer, S. Schuppler, Th. Fauster, and W. Steinmann, Surf. Sci. **314**, 89 (1994).
[7] L.-A. Salmi and M. Persson, Phys. Rev. B **39**, R6249 (1989).
[8] H. Ishida and K. Terakura, Phys. Rev. B **38**, R5752 (1988).
[9] H. Ishida, Phys. Rev. B **40**, R1341 (1989).
[10] E. V. Chulkov and V. M. Silkin, Surf. Sci. **215**, 385 (1989).
[11] G. A. Benesh and J. R. Hester, Surf. Sci. **194**, 567 (1989).
[12] A. Carlsson, S. Å. Lindgren, C. Svensson, and L. Walldén, Phys. Rev. B **50**, R8926 (1994).
[13] C. Stampfl, K. Kambe, R. Fasel, P. Aebi, and M. Scheffler, Phys. Rev. B **57**, 15251 (1998).
[14] J. M. Carlsson and B. Hellsing, Phys. Rev. B **61**, 13973 (2000).
[15] C. Stampfl and M. Scheffler, Surf. Rev. Lett. **2**, 317 (1995).
[16] M. Milun, P. Pervan, and D. P. Woodruff, Rep. Prog. Phys. **65**, 99 (2002).
[17] R. W. Gurney, Phys. Rev. **47**, 479 (1935).
[18] J. Burchhardt, M. M. Nielsen, D. L. Adams, E. Lundgren, J. N. Andersen, C. Stampfl, M. Scheffler, A. Schmalz, S. Aminpirooz,

and J. Haase, Phys. Rev. Lett. **74**, 1617 (1995).
[19] J. E. Inglesfield, J. Phys. C **14**, 3795 (1981).
[20] H. Ishida, Phys. Rev. B **63**, 165409 (2001).
[21] E. V. Chulkov, J. Kliewer, R. Berndt, V. M. Silkin, B. Hellsing, S. Crampin, and P. M. Echenique, Phys. Rev. B **68**, 195422 (2003).
[22] H. Ishida, Surf. Sci. **388**, 73 (1997).
[23] G. Butti, M. I. Trioni, and H. Ishida, Phys. Rev. B **70**, 195425 (2004).
[24] A. G. Eguiluz, M. Heinrichsmeier, A. Fleszar, and W. Hanke, Phys. Rev. Lett. **68**, 1359 (1992).
[25] G. Fratesi, G. P. Brivio, P. Rinke, and R. W. Godby, Phys. Rev. B **68**, 195404 (2003).
[26] M. Nekovee and J. E. Inglesfield, Europhys. Lett. **19**, 535 (1992).
[27] M. Nekovee and J. E. Inglesfield, Prog. Surf. Sci. **50**, 149 (1996).
[28] In particular, the mixing is performed in the so-called *near-surface region* which extends from the edge of the topmost muffin tin to the vacuum embedding surface.
[29] H. Ishida and A. Liebsch, Phys. Rev. B **66**, 155413 (2002).
[30] I. Merrick, J. E. Inglesfield, and G. A. Attard, Phys. Rev. B **71**, 085407 (2005).
[31] N. D. Lang and W. Kohn, Phys. Rev. B **7**, 3541 (1973).
[32] J. P. Perdew, K. Burke, and M. Ernzerhof, Phys. Rev. Lett. **77**, 3865 (1996).
[33] D. Tang, D. McIlroy, X. Shi, C. Su, and D. Heskett, Surf. Sci. **255**, L497 (1991).
[34] J. Kliewer and R. Berndt, Surf. Sci. **477**, 250 (2001).
[35] E. A. Colbourn and J. E. Inglesfield, Phys. Rev. Lett. **66**, 2006 (1991).
[36] W. Wallauer and Th. Fauster, Surf. Sci. **374**, 44 (1997).
[37] A. Carlsson, B. Hellsing, S. Å. Lindgren, and L. Walldén, Phys. Rev. B **56**, 1593 (1997).
[38] J. Kliewer and R. Berndt, Phys. Rev. B **65**, 035412 (2001).
[39] D. Wortmann, H. Ishida, and S. Blügel, Phys. Rev. B **65**, 165103 (2002).
[40] In order to check how this effect could affect our results, we performed several calculations for the clean Cu(111) surface, with an increasing number of layers enclosed in the embedded region. The energies of the SS fully converge considering four Cu layers inside the region, being only 15 meV higher than the reported one obtained with two layers. The inaccuracy related to the method constitutes therefore only a small fraction of the overall discrepancy with experiments.
[41] F. Forster, G. Nicolay, F. Reinert, D. Ehm, S. Schmidt, and S. Hüfner, Surf. Sci. **532-535**, 160 (2003).
[42] J. Kliewer, R. Berndt, E. V. Chulkov, V. M. Silkin, P. M. Echenique, and S. Crampin, Science **288**, 1399 (2000).
[43] M. Wolf, E. Knoesel, and T. Hertel, Phys. Rev. B **54**, R5295 (1996).
[44] P. M. Echenique, R. Berndt, E. V. Chulkov, Th. Fauster, A. Goldmann, and U. Höfer, Surf. Sci. Rep. **52**, 219 (2004).